energy&fuels

Article

pubs.acs.org/EF

Detailed Modeling of the Effects of K/Na Additives on the Thermal DeNO$_x$ Process

Xiaofeng Guo, Xiaolin Wei,* and Sen Li

State Key Laboratory of High Temperature Gas Dynamics, Institute of Mechanics, Chinese Academy of Sciences, Beijing 100190, People's Republic of China

ABSTRACT: A reduced mechanism simplified from a detailed chemical kinetics mechanism containing N/H/O/K/Na elements was developed and validated in this paper. When the reduced mechanism was integrated into computational fluid dynamics (CFD) software, the effect of potassium and sodium additives on the selective non-catalytic reduction (SNCR) thermal DeNO$_x$ process was simulated. The simulation results were compared to those of experiments under different oxygen concentrations, normalized stoichiometric ratios (NSRs) of the N agent/NO, and alkali metal additive concentrations within the temperature range from 1023 to 1523 K, and the simulation results coincided qualitatively with those of the experiment in an entrained flow reactor. The alkali metal additives did not change the effects of the oxygen concentration and NSR on the SNCR process: a conversion temperature point exists at about 1173−1223 K; below the conversion temperature point, a higher oxygen concentration can promote the effect of SNCR, while above the conversion temperature point, the efficiency will be reduced; and a higher NSR is beneficial for NO reduction, but its effect becomes less obvious with the increase of the reducing agent. The alkali metal additives extend the "temperature window" toward a lower temperature by about 50−100 K with more OH and NH_2 radical production, and the effect of K additives is less obvious than that of Na. However, the promoting effect of the K additive cannot be well-simulated because of the lack of a suitable mechanism. A K chemistry mechanism should be optimized on the basis of its effect on the SNCR process. The K or Na concentration almost has no influence on the effect of alkali metal additives on the thermal DeNO$_x$ process when the K or Na concentration is beyond a certain value.

1. INTRODUCTION

Nitrogen oxide (NO$_x$) produced during the combustion process has serious negative effects on the environment. As one of the main sources of NO$_x$, the thermal power generation process pays more attention to the technology of nitrogen removal because of the increasingly stringent emission standards for pollutants. Some technologies have been developed to reduce NO$_x$ emissions, which can be divided into two main categories: combustion control (including air staging, fuel staging, and flue gas recirculation) and flue gas treatment [including selective catalytic reduction (SCR), selective non-catalytic reduction (SNCR), non-selective catalytic reduction (NSCR), pulsed corona discharge, and electron beam flue gas treatment].[1] SNCR is an economic and effective flue gas post-processing technology for nitrogen removal,[2] through which the nitrogen-reducing agent is injected into the NO$_x$-containing flue gas at a convenient temperature (about 1250 K) and reduces NO$_x$ without a catalyst. The efficiency of SNCR in laboratory and power station can reach about 80−90 and 40−70%, respectively.[3] According to the different nitrogen-reducing agents, the SNCR process can be divided into three categories: the thermal DeNO$_x$ process (NH_3 as a reducing agent), the NO$_x$OUT process [$(NH_2)_2CO$ as a reducing agent], and the RAPRENO$_x$ process [$(HOCN)_3$ as a reducing agent].[4]

However, it is hard to gain the best nitrogen removal efficiency with pure application of SNCR because of the narrow "temperature window": when the temperature is low (lower than 1073 K), the nitrogen-reducing agent is not completely converted to N_2 and "ammonia slip" is easy to occur; when the temperature is high (higher than 1323 K), some of the reducing agent will be oxidized to NO$_x$. Some researchers are trying to gain a wider temperature window and higher nitrogen removal efficiency with various additives. Gas additives, such as CO, H_2, CH_4 or even complicated organic compounds, such as amines and alcohols, have been studied, and the results show that the optimal reaction temperature can be decreased by about 100 K or more and lower NH_3 slip can be obtained.[5−8] However, some researchers pointed out that the gas additives might increase the emission of harmful gas, such as CO and N_2O, and NO$_x$ reduction efficiency was also impaired.[7,8] Trace quantities of sodium salts can also extend the temperature window toward lower temperatures and will not cause the increase of the emission of harmful gas, which attract the attention of some researchers. Zamansky et al.[4] found that adding small amounts of sodium salts significantly improved the performance of the SNCR process through experiment and established a Na−O−H−N detailed mechanism combined with the research by Perry and Miller.[9] Lee et al.[10] pointed out that the efficiency of reduction of NO increased with all sodium additives but descended in the order NaOH, Na_2CO_3, $NaNO_3$, HCOONa, and CH_3COONa. Yang et al.[11] obtained the conclusions that the effect of different Na_2CO_3 concentration additives was nearly the same and sodium enhanced the OH radical concentration mainly through the following reactions: NaO + H_2O = NaOH + OH, NaOH + O_2 = NaO_2 + OH, and NaOH + M = Na + M + OH, on the basis of the urea-SNCR process. Niu et al.[3] studied the NO$_x$OUT process and found that the efficiency improved obviously when the NaOH

Received: August 27, 2012
Revised: November 19, 2012
Published: November 20, 2012

dx.doi.org/10.1021/ef3014037 | *Energy Fuels* 2013, 27, 421−429

additive increased from 10 to 20 ppm but further increasing the additive concentration made little sense.

Some important conclusions have been obtained through previous studies. However, most of them focus on the influence of sodium additive, and the results are obtained from experiments or some ideal reactor models, such as perfectly stirred reactor (PSR) and plug flow reactor (PFR). With the shortage of traditional fossil fuel in the immediate future, biomass has been increasingly widely used as the main or reburning fuel because of its advantages, such as low nitrogen content, high volatile content, carbon-neutral fuel, wide source, and little investment in technological improvement on the existing boiler. Besides sodium, potassium is also an alkali metal element rich in biomass. While combusting, biomass will release tens of parts per million concentration of potassium species into the flue gas, which has attracted almost no attention and research on its effect on SNCR.

Therefore, the aim of the present work is to develop a chemical reaction model, research the effect of potassium species on the nitrogen removal process by numerical simulation and experiment, and figure out the similarity and difference between potassium and sodium on nitrogen removal efficiency. With the development of a reduced mechanism containing K/Na elements from a detailed one using a self-written and two open-source programs and integration of it into computational fluid dynamics (CFD) software, the effect of potassium and sodium additives on the SNCR process is studied and compared to experimental results under different oxygen concentrations, normalized stoichiometric ratios (NSRs) of the N agent/NO, and alkali metal additive concentrations within the temperature range from 1023 to 1523 K. Because both of the SNCR processes for the thermal $DeNO_x$ and NO_xOUT reduce NO_x through NH_3 obtained by direct injection or indirect decomposition, the present work focuses on the effect of NH_3 and the research is based on the thermal $DeNO_x$ process.

2. MECHANISM REDUCTION AND VALIDATION

The reduction and validation of the mechanism were obtained by the following steps: (1) set up a detailed mechanism that can describe well the problem being researched; (2) establish a skeletal mechanism through deleting redundant species and reactions in the selected conditions; (3) develop a reduced mechanism by quasi-steady-state (QSS) assumption based on elimination of QSS species; and (4) validate the accuracy of the reduced mechanism against the detailed one under the whole range of selected conditions.

The present mechanism reduction procedure was performed on the basis of the SENKIN model,[12] which solves the conservation equations for mass and energy and calculates the temporal evolution of molar fractions of species for a homogeneous mixture. Because the temperature was almost constant in the research, a reactor system with a constant pressure and temperature was selected. For mechanism reduction, a self-written program combined with two open-source programs KINALC and MECHMOD[13] was used. KINALC can analyze the gas kinetic mechanism by reading the concentrations and sensitivities calculated by SENKIN, including 17 different methods for the analysis of the complex reaction mechanism. MECHMOD is an auxiliary program that can modify the mechanism, such as changing of units, elimination of species, changing a reversible reaction to pairs of irreversible reactions, etc. More information about them can be gained from ref 14.

2.1. Detailed Mechanism. To evaluate the effects of potassium and sodium additives on the thermal $DeNO_x$ process, a detailed mechanism containing N/H/O/K/Na elements should be set up first. In the present work, the ÅA mechanism was selected as a basic reaction model, which was established by Zabetta et al.[15] and can predict the SNCR process well. For alkali metal elements, the K and Na mechanisms proposed by Hindiyarti et al.[16] and Zamansky et al.[4], respectively, were used to describe the behavior of alkali metal additives and species. Because of the similar character of congeners, we assumed that alkali metal additives rapidly converted to hydroxide according to ref 4; therefore, KOH and NaOH were treated as the initial reactants in the simulation. To coincide with the experiments, only N/H/O/K/Na species were retained; the C-, S-, and Cl-containing species in the original mechanism were omitted, because they were not present in the experiments modeled. Finally, a detailed mechanism was set up, including 35 species and 368 irreversible elementary reactions, using MECHMOD.

2.2. Skeletal Mechanism. The skeletal mechanism was derived by eliminating unimportant species and reactions using the CONNECT and sensitivity analysis (SA) methods, both of which are encoded in KINALC and introduced in detail in ref 14. The reduction procedure was based on the experimental conditions as follows: T = 1023−1523 K; p = 0.1 MPa; $[O_2]$ = 2−4%; $[H_2O]$ = 6%; [NO] = 400 ppm; NSR = 1.2−2.1; [KOH] and [NaOH] = 0−50 ppm; N_2 as balance gas; and the reaction time = 500 ms. All of the concentrations are on the volume basis in the experiment and simulation of this paper.

First, the CONNECT method was used to find redundant species by choosing NO, NH_3, O_2, NaOH, KOH, and N_2 as the main species. After analysis, eight species were found redundant during the whole reaction time and eliminated from the detailed mechanism. Then, the SA method was taken for the remaining mechanism, with a predefined criterion as 0.1%. After calculation, the reactions with normalized sensitivity coefficients smaller than this criterion were eliminated; therefore, the skeletal mechanism was obtained, including 27 species and 137 irreversible reactions, shown in the Appendix.

2.3. Reduced Mechanism. On the basis of the same reaction conditions, the QSS analysis method[14] was taken to identify QSS species, whose production and consumption rates are nearly the same and whose net reaction rates are assumed to be zero according to the QSS assumption. With this method in KINALC, 13 species were identified as QSS species. To represent the stoichiometry of the overall skeletal chemical system by a reduced mechanism, an independent set of reaction steps from the skeletal mechanism should be selected and used to eliminate the QSS species according to the matrix operation of mechanism reduction and the QSS assumption. To ensure the smallest errors, the elimination always selected the least sensitive reactions in the skeletal mechanism involving each specific QSS species; in this paper, they were H-w3, O-w43, HO_2-w125, NH-w75, NNH-w74, N_2H_2-w71, HNO-w48, HONO-w57, H_2NO-w61, KO-w107, KO_2-w104, NaO-w116, and NaO_2-w136. A self-written program was used to automatically read the skeletal mechanism, QSS species, and reactions to be eliminated and, through a series of operations, write out the report file, including the whole information of the reduced mechanism. For the present work, the reduced mechanism involves 14 species and 9 reactions.

$$2NH_3 \Rightarrow 2NH_2 + H_2 \quad (1)$$

$$NH_3 + NO + O_2 \Rightarrow NH_2 + NO_2 + OH \quad (2)$$

$$NH_3 + OH \Rightarrow NH_2 + H_2O \quad (3)$$

dx.doi.org/10.1021/ef3014037 | Energy Fuels 2013, 27, 421−429

$$NH_2 + NO_2 \Rightarrow H_2 + O_2 + N_2 \quad (4)$$

$$NH_3 + NO + 2O_2 \Rightarrow 2NO_2 + OH + H_2 \quad (5)$$

$$2NH_2 + O_2 \Rightarrow NH_3 + NO + OH \quad (6)$$

$$NH_2 + NO_2 \Rightarrow N_2O + H_2O \quad (7)$$

$$NO + O_2 + H_2O + K \Rightarrow NO_2 + OH + KOH \quad (8)$$

$$NO_2 + H_2O + Na \Rightarrow NO + OH + NaOH \quad (9)$$

For each reaction in the reduced mechanism, the reaction rate is expressed in terms of the elementary reaction rates in the skeletal mechanism as provided in Table 1.

2.4. Validation of the Reduced Mechanism. The SENKIN model was also used to validate the reduced mechanism. Because the reaction rate of each species in the reduced mechanism is not a single Arrhenius expression any more, the subroutine for calculating the production rate of each species should be modified to express the reaction rate of the reduced mechanism. The validation was based on the experimental and simulated conditions and covered the main variation range of parameters. The calculated result of the reduced mechanism was compared to that of the detailed and skeletal mechanisms from different aspects, as shown in Figures 1 and 2.

Figure 1a shows the NO and NH_3 concentrations calculated with different mechanisms with the change of time. The skeletal mechanism coincides well with the detailed mechanism, while the reduced mechanism is slightly lower. However, the largest relative error is no more than 5%, and the error is only obvious at the beginning of the reaction time (0−200 ms), after which the reduced mechanism coincides well with the detailed mechanism. Figure 1b is the calculated result for two important free radicals OH and NH_2. In the range of 0−100 ms, the concentrations of OH and NH_2 calculated by the reduced mechanism are slightly higher, while after this time, the three mechanisms coincide well. The overestimated production of OH and NH_2 at the beginning is the main reason for the deviation of NO and NH_3 for the reduced mechanism.

Figure 2 is the comparison results of the NO concentration at the end of the reaction time with different mechanisms. It indicates that the reduced mechanism can predict well the final NO molar fraction against the detailed mechanism at different oxygen concentrations and NSRs. Because the deviation for main species and free radicals is not large and within the allowable error and the NO concentration at the outlet that we concern most is well-coincident with the detailed mechanism, this reduced mechanism will be used in the following CFD simulations.

Table 1. Reaction Rate Expressed in Terms of the Elementary Reaction Rates in the Skeletal Mechanism

W_1 = w1 − w21 − w22 − w32 − w34 + w35 − w36 + w37 − w44 + w45 − w46 + w60 + w69 − w76 − w78 − w80 − w88 + w89 − w90 + w91 + w101 − w102 + w105 − w108 + w109 − w111 + w112 − w119 + w120 − w121 + w122

W_2 = w4 − w5 + w10 − w13 + w14 − w17 − w19 + w20 + w21 + w22 − w26 − w27 − w30 − w31 + w32 − w36 + w37 + w40 − w41 − w45 + w46 − w47 − w49 + w50 − w52 + w53 − w54 − w55 + w62 + w63 + w65 − w66 + w76 + w78 + w79 + w80 − w81 + w82 + w83 − w86 + w87 + w88 − w89 + w90 − w91 − w92 + w93 − w96 + w97 − w99 + w100 − w101 + w102 − w105 + w108 − w109 − w110 + w111 − w112 − w119 + w120 − w121 + w122 − w123 + w124 − w127 + w128 − w129 + w130 − w131 + w134 − w135

W_3 = w6 − w7 + w11 + w21 + w22 − w30 − w31 − w33 + w36 − w37 + w49 − w50 + w54 + w58 + w59 + w64 + w68 + w70 − w72 + w73 + w79 + w80 + w84 − w85 + w86 − w87 + w96 − w97 + w99 − w100 + w101 − w102 − w105 + w110 + w111 − w112 + w119 − w120 + w121 − w122 + w123 − w124 + w127 − w128 + w129 − w130 + w131 + w132 − w133

W_4 = w8 + w10 + w11 + w17 + w18 + w20 + w21 + w22 − w26 − w27 − w28 − w29 − w30 − w31 − w33 + w58 − w72 + w73 + w79 + w80 + w111 − w112

W_5 = w9 + w17 + w19 + w26 + w27 + w30 + w31 + w34 − w35 + w36 − w37 − w40 + w41 + w44 − w62 − w79 + w81 − w82 − w93 − w101 + w102 + w119 − w120 + w121 − w122 − w134 + w135

W_6 = w12 − w15 + w16 + w24 − w25 + w28 + w29 − w30 − w31 − w34 + w35 − w36 + w37 + w40 − w41 − w44 − w55 − w72 + w73 + w79 − w81 + w82 + w93 + w101 − w102 − w119 + w120 − w121 + w122 + w134 − w135

W_7 = w23 + w30 + w31 + w33 + w55 + w72 − w73 − w79 − w80 − w111 + w112

W_8 = w98 + w99 − w100 + w101 − w102 + w105 − w108 + w109 + w110

W_9 = w113 − w114 + w119 − w120 + w121 − w122 + w123 − w124 + w127 − w128 + w129 − w130 + w131 + w132 − w133 − w134 + w135

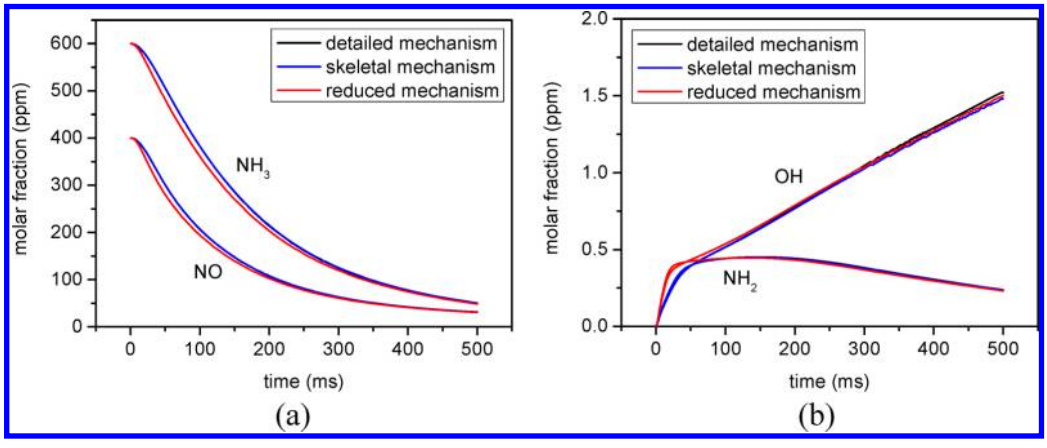

Figure 1. Comparison of the reduced mechanism with the detailed and skeletal mechanisms at different times (T = 1173 K; [NO] = 400 ppm; [O_2] = 3%; [KOH] and [NaOH] = 50 ppm; NSR = 1.5; and [H_2O] = 6%).

dx.doi.org/10.1021/ef3014037 | Energy Fuels 2013, 27, 421−429

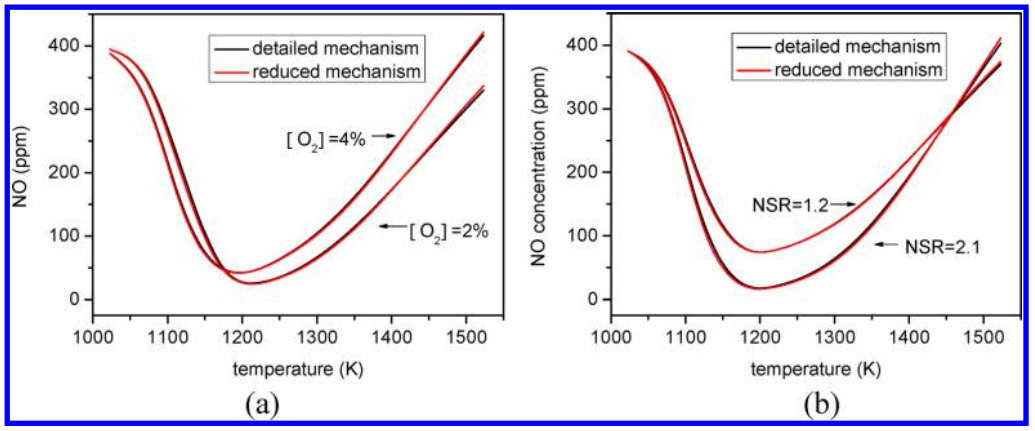

Figure 2. Comparison of the reduced mechanism with the detailed mechanism for different temperatures at (a) different oxygen concentrations (NSR = 1.5) and (b) different NSRs ($[O_2]$ = 3%) ([NO] = 400 ppm; [KOH] and [NaOH] = 50 ppm; and $[H_2O]$ = 6%).

3. DESCRIPTION OF THE EXPERIMENTAL AND SIMULATION METHODS

3.1. Experimental System and Method. The experiments and simulations were executed for an electrically heated entrained flow reactor (EFR), with a height of 1.93 m and an inner diameter of 70 mm, and the system is shown in Figure 3. The EFR has three regulated

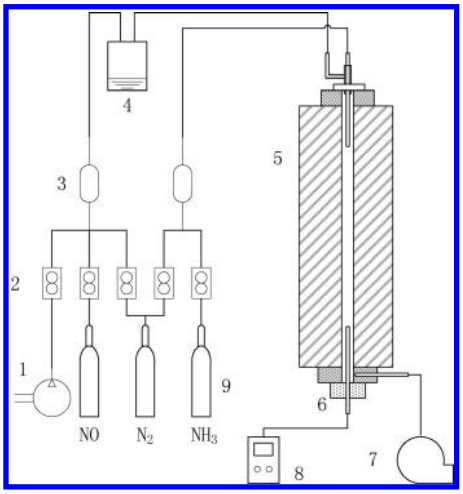

Figure 3. Schematic of the experimental system: (1) air compressor, (2) mass flow controller, (3) mixing tank, (4) atomizer, (5) EFR, (6) water-cooling gas probe, (7) draft fan, (8) gas analyzer, and (9) gas cylinder.

heating zones, with a maximum temperature of 1873 K, measured by PtRh−Pt thermocouples. The oxygen needed in the experiments is supplied by an air compressor, while the nitrogen is supplied by both an air compressor and a gas cylinder. NO and NH_3 come from standard gas with 5% concentration. Each flow is exactly controlled by a mass flow controller. The first flow mixed by O_2, N_2, and NO is sent into the EFR, carrying the atomized alkali metal liquid solution, with a diameter of 1−5 μm. The second flow mixed by N_2 and NH_3 is sent deep into the reactor by 0.4 m through a corundum tube, and the length of reaction district is 1.2 m. The NO molar fraction is measured online by a gas analyzer through a gas probe cooled by water from the bottom of the reactor. The gas analyzer is ECOM-J2KN, with the NO measuring range of 2000 ppm and precision of ±5 ppm. To ensure its accuracy, the gas analyzer is calibrated everyday before the experiments. Besides, to maximally exclude the interference caused by alkali metal deposition on the inner wall, a large quantity of air is pumped into the reactor under the temperature of 1773 K for 1 h everyday before the experiments, vaporizing the deposit and blowing it out of the reactor.

In the experiments, the total volumetric flow rate is 15 NL/min and the residence time is about 3−4 s to ensure that the reaction of SNCR goes to completion. The total flow can be divided into two main flows. The first flow rate is kept at 13 N L min^{-1}, and the NO molar fraction is about 400 ppm. When tests and calibrations are repeated before the experiments, this gas flow rate can carry atomized solution of about 0.6 g/min. If all H_2O and alkali metal additives are assumed to completely evaporate, the H_2O molar fraction is about 6%. Therefore, the alkali metal concentration can be controlled accordingly when preparing the alkali metal solution. The second flow is kept at 2 NL/min, changing NSR by adjusting the NH_3 mixing ratio. In the present experiments, the effects of K and Na additives on the thermal $DeNO_x$ process were studied under different temperatures (1023−1523 K), oxygen concentrations (2.0, 2.8, and 3.7%), NSRs (1.2, 1.5, 1.8, and 2.1), and atom concentrations of alkali metal (0, 25, and 50 ppm). The alkali metal salts used were K_2CO_3 and Na_2CO_3, which have two alkali metal atoms in each molecule. The experimental data were recorded after being kept stable for about 2 min, and each experimental point was an average result of two measurements.

3.2. Numerical Simulation Method. The effects of alkali metal additives on the thermal $DeNO_x$ process were simulated by FLUENT software in the present work. Through user-defined function (UDF), the reduced mechanism can be integrated into this CFD program and save much time, because the time required for the simulation is approximately proportional to the number of elementary reactions and the square or cube of the number of species. To further reduce computing time, the numerical model was assumed to be two-dimensional (2D) axial symmetric and the size was the same as that of the EFR. The computational area was discretized with a rectangular grid, and the inlet and main reacting areas were properly densified. All of the initial and boundary conditions were set according to the experiments with a constant wall temperature assumption. Because the velocity on the inlet of the second flow is 30−40 times larger than that of the first flow and turbulence always exists in the experiments, a low Reynolds $k-\varepsilon$ model established by Launder and Sharma[17] was used for the turbulence simulation. The SIMPLE method was used to solve the velocity and pressure coupling, and the eddy dissipation concept (EDC)[18] model was for calculating the interaction between turbulence and chemistry reactions. Besides, the *in situ* adaptive tabulation (ISAT)[19] method was applied to accelerate the computation of the reaction rates, which can greatly reduce the computational consumption. Because of the high temperature of the reactor and small atomized particle size of the alkali metal liquid solution, the alkali metal additives were assumed to be completely vaporized into the gas phase; therefore, all of the reactions in the simulation are homogeneous, and the reduced mechanism can be used in the simulation.

4. MODELING RESULTS AND COMPARISON TO EXPERIMENTS

On the basis of the reduced mechanism modeling, the effects of potassium and sodium additives on the thermal $DeNO_x$ process in various conditions were simulated and compared to the

dx.doi.org/10.1021/ef3014037 | *Energy Fuels* 2013, 27, 421−429

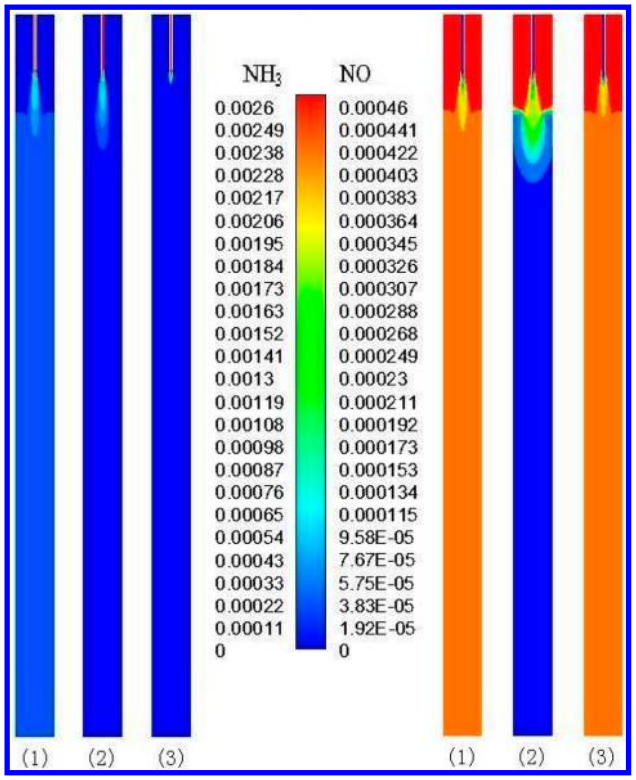

Figure 4. Simulation result of the distribution of NH_3 and NO mass fractions under different temperatures: (1) 1073 K, (2) 1273 K, and (3) 1473 K.

experimental results. In these results, the temperature shows the most obvious effect on the NO_x removal process. In Figure 4, the distribution of NH_3 and NO mass fractions is presented, where the process shows different characteristics with various temperatures. At a low temperature of 1073 K, the NH_3-reducing agent does not react very much and equally distributes, which causes low NO_x removal efficiency and high ammonia slip. A convenient temperature, such as 1273 K, is beneficial for the reaction of N agents. The effect is obvious, and there is nearly no ammonia found at the exit. However, at the high temperature of 1473 K, NH_3 is easily oxidized rapidly to NO_x, the rate of which is faster than that of the reducing reaction; therefore, the efficiency is low. The model reproduces the effect of the temperature on SNCR satisfactorily and indicates that the simulation results are reasonable.

In Figures 5, 7, and 8, where NO_{out} and NO_0 represent the NO molar fraction at the exit of the reactor with and without NH_3-reducing agent, respectively, the simulation result under various conditions coincides with that of the experimental result qualitatively. Limited by the precision of the experiment, both the simulation and experimental results are quantitatively identical only at the temperature from 1173 to 1373 K, below or above which the experiment shows better effects on NO_x removal. On the one hand, the deviation may be caused by some experimental factors, such as air leakage, alkali metal deposition, surface reactions of the reactor wall, non-uniform temperature and concentration field, liquid solution atomization, and alkali metal additive decomposition and vaporization. On the other hand, aspects of the model may also cause the deviation, such as

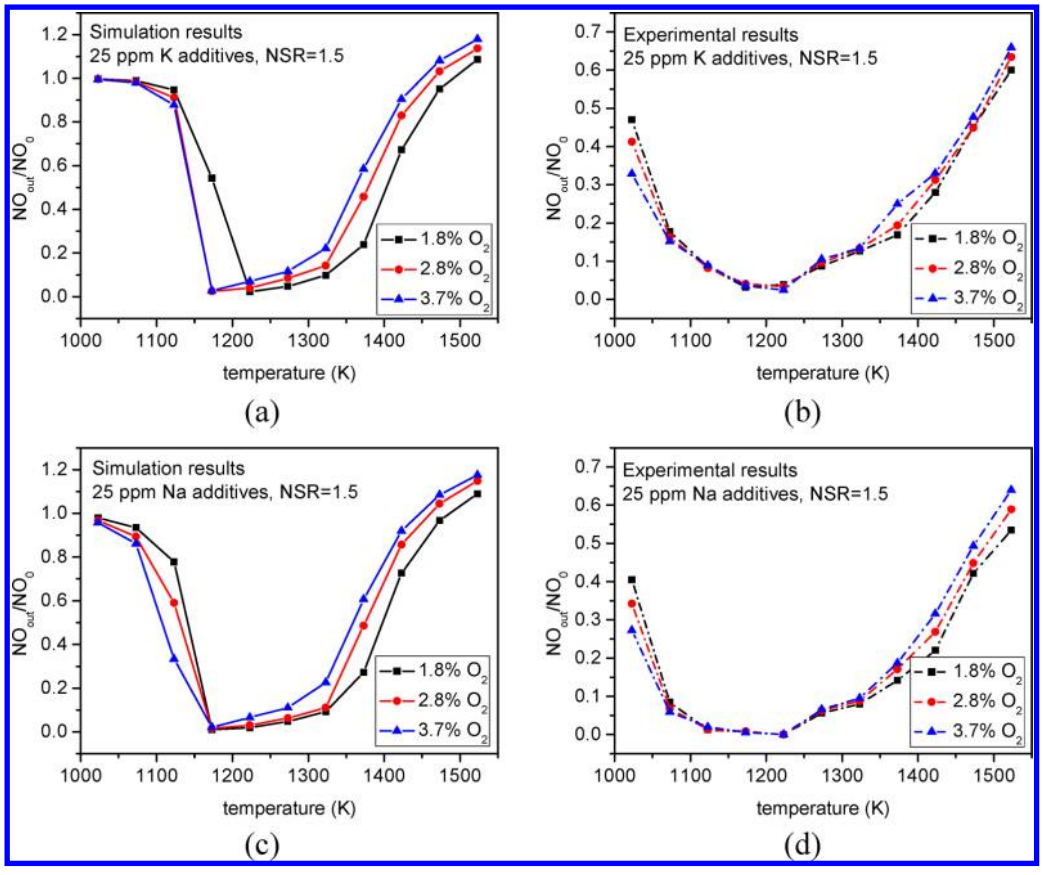

Figure 5. Simulation and experimental results of different oxygen concentrations with alkali metal additives: (a and b) K additive and (c and d) Na additive.

dx.doi.org/10.1021/ef3014037 | *Energy Fuels* 2013, 27, 421−429

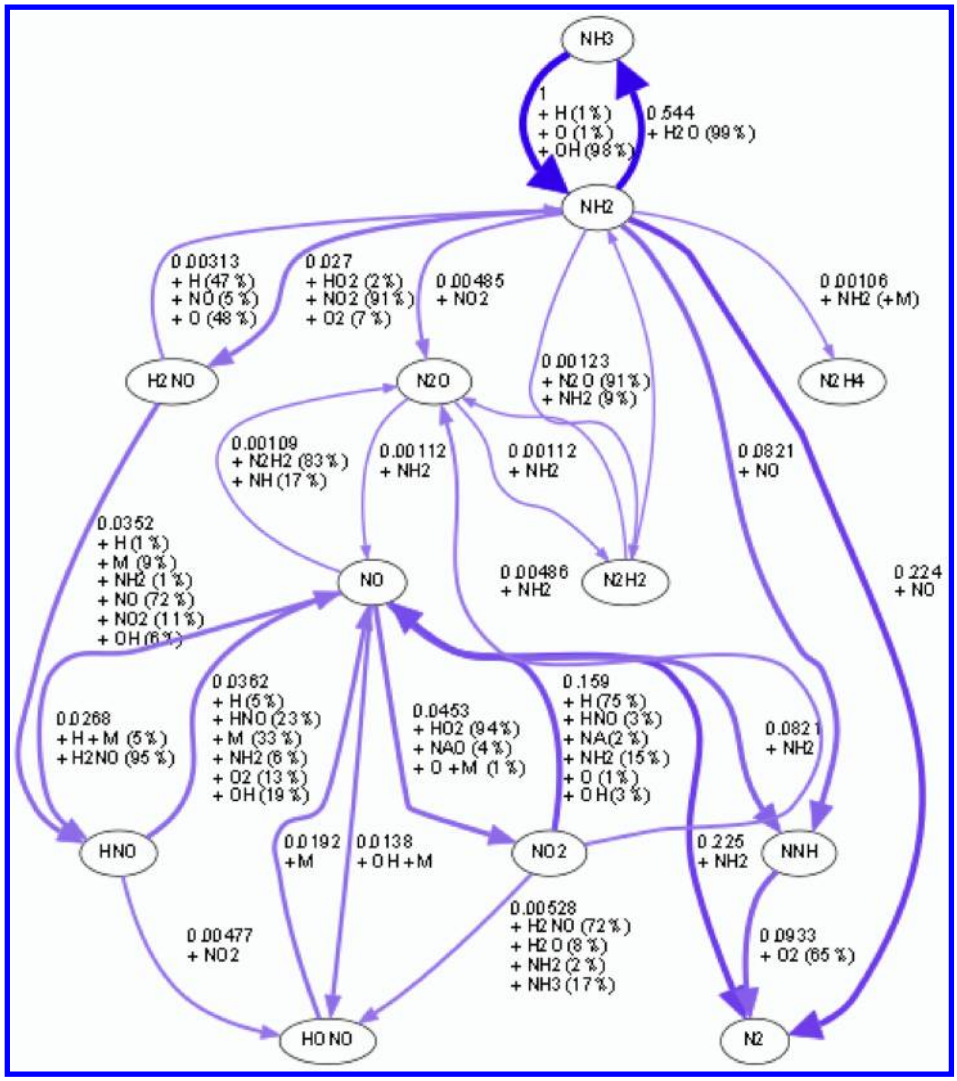

Figure 6. Reaction path analysis for N species ([NO] = 400 ppm; [O_2] = 3%; [KOH] and [NaOH] = 25 ppm; and NSR = 1.5).

uncertainty of rate constants for some reactions containing alkali metals. Besides, in the work by Mahmoudi et al. researching SNCR on biomass combustion, similar DeNO$_x$ efficiency was obtained in laboratory and large-scale experiments,[1] which indicates that the experimental data in this paper are reasonable. Therefore, the experimental data are used to compare to the modeling results qualitatively in the present work, which can also well-illustrate the changing trend in different conditions.

Figure 5 is the result for different oxygen concentration conditions at NSR = 1.5, which indicates that the effect of oxygen is variable within the temperature range and the K and Na additives do not change this phenomenon compared to the result without additives in our research and others' work.[11] A conversion temperature point exists at about 1173−1223 K in both simulation and experiment. Below this point, a higher oxygen concentration can promote the effect of SNCR, while above it, the efficiency will be reduced. The reaction path is analyzed on the basis of the plug flow model using Cantera,[20] as shown in Figure 6. Because NO is reduced mainly through two paths: (1) $NH_2 + NO \rightarrow N_2 + H_2O$ and (2) $NH_2 + NO \rightarrow NNH + OH$ and $NNH + O_2 \rightarrow N_2 + HO_2$, NH_2 is acting as a reducing agent in the NO$_x$ removal process, which is mainly produced by reaction $NH_3 + OH \rightarrow NH_2 + H_2O$. At lower temperatures, high concentrations of oxygen can promote the production of OH; therefore, more NH_2 can form to reduce NO. At higher temperatures, enough OH radical is produced by H_2O. Oxygen is an important oxidant of NH_3 in this condition; therefore, the efficiency of SNCR becomes lower.

Figure 7 compares simulation and experimental results under different NSR conditions at 2.8% oxygen concentration, and it can be concluded that a higher NSR is beneficial for the NO reduction; however, the promoting effect becomes less obvious with the increase of the reducing agent. In the experiment, higher NSR promotes the effect in the whole range of temperatures, while this promoting effect disappears above 1373 K in the simulation and reduces the efficiency of SNCR, with more NH_3 being oxidized under high temperatures as a possible reason. Despite the difference, both results show that NSR = 1.5 is appropriate for reducing NO, above which more NH_3 cannot show a further promoting effect. As a result, the cost of the reducing agent must be considered in the actual production process to gain a relatively high efficiency. Similar to that of the oxygen concentration, the alkali metal additives do not change the effect of NSR.

However, the alkali metal additives indeed change the range of the "temperature window" and promote the efficiency of SNCR to some extent, especially for Na additives, which is shown in

dx.doi.org/10.1021/ef3014037 | Energy Fuels 2013, 27, 421−429

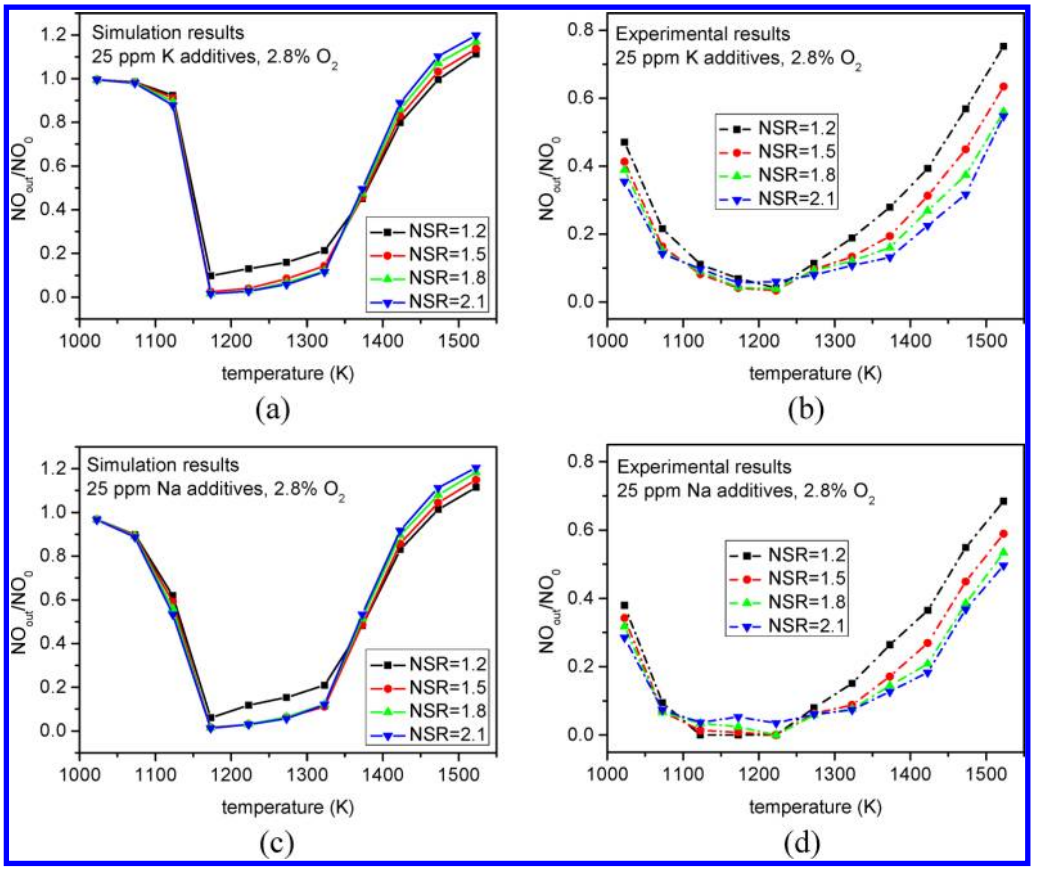

Figure 7. Simulation and experimental results of different NSRs with alkali metal additives: (a and b) K additive and (c and d) Na additive.

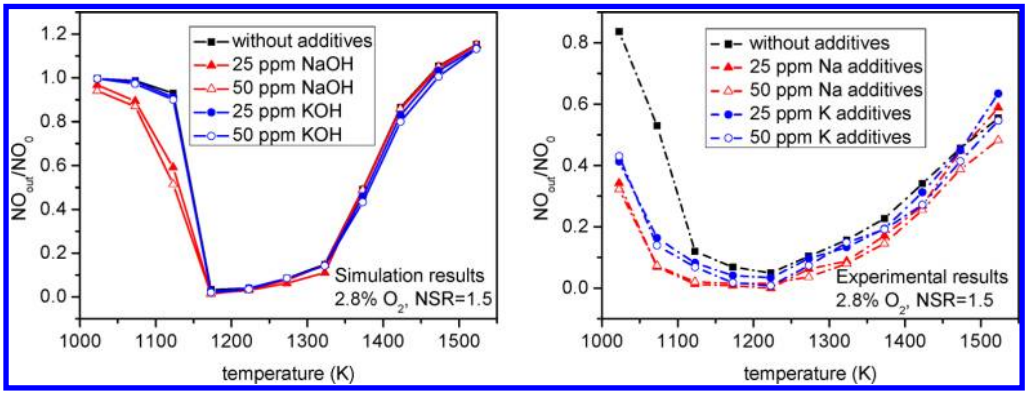

Figure 8. Simulation and experimental results of the comparison of alkali metal additives on the thermal DeNO$_x$ process.

Figure 8. Both simulation and experimental results indicate that the "temperature window" extends toward the lower temperature by about 50−100 K, with efficiency promotion by Na additives. From Figure 9, it can be seen that the OH mass fraction is increased after adding Na additive at 1123 K, which is caused by the promoting effect of NaOH + O_2 ⇒ NaO_2 + OH, NaOH + M ⇒ Na + OH + M, and NaO + H_2O ⇒ NaOH + OH on OH radical production through reaction path and sensitivity analysis. Therefore, the alkali metal additive enhances the production of OH, which promotes the NH_2 production to reduce NO, and this can also be seen in the simulation result shown in Figure 9. However, for K additives, only a slight promoting effect is observed in the simulation at low temperatures, which is not well-coincident with the experimental result in Figure 8. In the experiment, although the effect of K additives is less than that of Na, the improvement of the efficiency is still obvious, and Lissianski et al.[21] also found an obvious promoting effect for K additives in their research. A possible reason is that, although the form of the main reaction in the Na mechanism also exists in the K mechanism, the K mechanism was established and optimized for the research of alkali metal aerosol formation during biomass combustion and the mechanism may be not very suitable for describing the influence of K additives in the SNCR process. Li et al.[22] pointed out that the reaction rate constant of K + OH = KOH is only $^1/_{64}$ of Na + OH = NaOH; therefore, KOH has low promotion of NO reduction compared to NaOH in the biomass-reburning process while researching with the same alkali metal reaction mechanism, and this may be possible to explain the obviously different promoting effects between K and Na additives in our simulation.

From the results with alkali metal additives in Figure 8, another conclusion can be obtained that the Na and K

dx.doi.org/10.1021/ef3014037 | Energy Fuels 2013, 27, 421−429

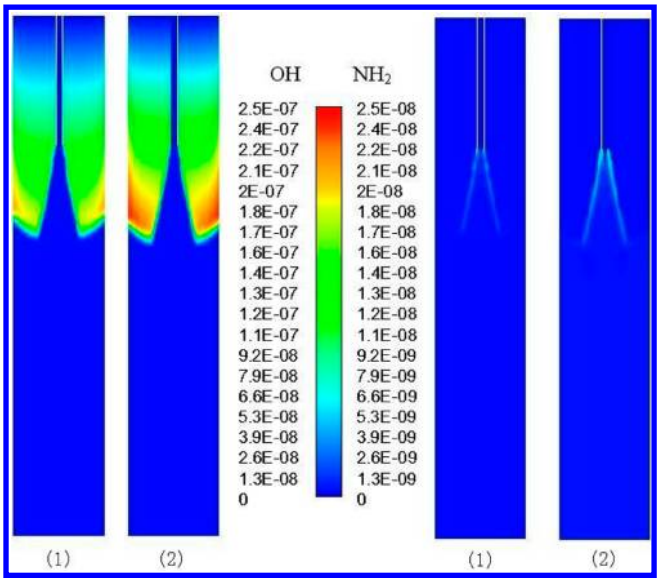

Figure 9. Simulation result of the distribution of OH and NH_2 mass fractions at 1123 K at the initial segment of the reactor (1) clean reactor (2) reactor with 25 ppm Na additive.

concentrations almost have no influence on their effect on the thermal $DeNO_x$ process, for which the simulation and experimental results coincide well. Once added beyond a certain concentration (20 ppm for Na by Niu et al.[3]), K or Na additives will show almost the same promoting effect on the SNCR process.

5. CONCLUSION

In the present work, a detailed mechanism was established to investigate the effects of K and Na additives on the thermal $DeNO_x$ process. With KINALC and MECHMOD open-source programs and a self-written code, a reduced mechanism was developed, validated, and integrated into CFD software to simulate the SNCR process. In comparison to the experimental results, the conclusions can be obtained as follows: (1) Alkali metal additives do not change the effect of the oxygen concentration on the SNCR process. A conversion temperature point exists at about 1173−1223 K. Below this point, higher oxygen concentrations can promote the effect of SNCR, while above it, the efficiency will be reduced. (2) A higher NSR is beneficial for the NO reduction, but its effect becomes less obvious with the increase of the reducing agent. NSR = 1.5 is appropriate in the present work, and the K and Na additives also do not change this conclusion. (3) The alkali metal additives extend the "temperature window" toward lower temperatures by about 50−100 K with more OH and NH_2 radical production, and the effect of K additives is less than that of Na additives. However, the promoting effect of K additives cannot be well-simulated because of the lack of a suitable mechanism; therefore, a K chemistry mechanism should be optimized on the basis of its effect on the SNCR process. (4) The K or Na concentration has almost no influence on the effect of alkali metal additives on the thermal $DeNO_x$ process when the K or Na concentration is beyond a certain value.

APPENDIX

Reactions of the skeletal mechanism are provided in Table A1.

Table A1. Reactions of the Skeletal Mechanism

1: $NH_3 + M \Rightarrow NH_2 + H + M$
2: $NH_3 + H \Rightarrow NH_2 + H_2$
3: $NH_2 + H_2 \Rightarrow NH_3 + H$
4: $NH_3 + O \Rightarrow NH_2 + OH$
5: $NH_2 + OH \Rightarrow NH_3 + O$
6: $NH_3 + OH \Rightarrow NH_2 + H_2O$
7: $NH_2 + H_2O \Rightarrow NH_3 + OH$
8: $NH_2 + H \Rightarrow NH + H_2$
9: $NH_2 + O \Rightarrow HNO + H$
10: $NH_2 + O \Rightarrow NH + OH$
11: $NH_2 + OH \Rightarrow NH + H_2O$
12: $NH_2 + HO_2 \Rightarrow H_2NO + OH$
13: $NH_2 + HO_2 \Rightarrow NH_3 + O_2$
14: $NH_3 + O_2 \Rightarrow NH_2 + HO_2$
15: $H_2NO + O \Rightarrow NH_2 + O_2$
16: $NH_2 + O_2 \Rightarrow H_2NO + O$
17: $2NH_2 \Rightarrow N_2H_2 + H_2$
18: $2NH_2 \Rightarrow NH_3 + NH$
19: $NH_2 + NH \Rightarrow N_2H_2 + H$
20: $NH_2 + NO \Rightarrow NNH + OH$
21: $NH_2 + NO \Rightarrow N_2 + H_2O$
22: $NH_2 + NO \Rightarrow N_2 + H_2O$
23: $NH_2 + NO_2 \Rightarrow N_2O + H_2O$
24: $NH_2 + NO_2 \Rightarrow H_2NO + NO$
25: $H_2NO + NO \Rightarrow NH_2 + NO_2$
47: $HNO + H \Rightarrow NO + H_2$
48: $HNO + O \Rightarrow NO + OH$
49: $HNO + OH \Rightarrow NO + H_2O$
50: $NO + H_2O \Rightarrow HNO + OH$
51: $HNO + O_2 \Rightarrow NO + HO_2$
52: $HNO + NH_2 \Rightarrow NO + NH_3$
53: $NO + NH_3 \Rightarrow HNO + NH_2$
54: $HNO + NO_2 \Rightarrow HONO + NO$
55: $2HNO \Rightarrow N_2O + H_2O$
56: $HONO + OH \Rightarrow NO_2 + H_2O$
57: $NO_2 + H_2O \Rightarrow HONO + OH$
58: $NH_2 + NO_2 \Rightarrow HONO + NH$
59: $NH_3 + NO_2 \Rightarrow HONO + NH_2$
60: $H_2NO + M \Rightarrow HNO + H + M$
61: $H_2NO + H \Rightarrow HNO + H_2$
62: $H_2NO + H \Rightarrow NH_2 + OH$
63: $H_2NO + O \Rightarrow HNO + OH$
64: $H_2NO + OH \Rightarrow HNO + H_2O$
65: $H_2NO + NO \Rightarrow 2HNO$
66: $2HNO \Rightarrow H_2NO + NO$
67: $H_2NO + NH_2 \Rightarrow HNO + NH_3$
68: $H_2NO + NO_2 \Rightarrow HONO + HNO$
69: $N_2H_2 + M \Rightarrow NNH + H + M$
70: $N_2H_2 + OH \Rightarrow NNH + H_2O$
71: $N_2H_2 + NH_2 \Rightarrow NNH + NH_3$
93: $HO_2 + H \Rightarrow 2OH$
94: $HO_2 + O \Rightarrow OH + O_2$
95: $OH + O_2 \Rightarrow HO_2 + O$
96: $HO_2 + OH \Rightarrow H_2O + O_2$
97: $H_2O + O_2 \Rightarrow HO_2 + OH$
98: $K + O + M \Rightarrow KO + M$
99: $K + OH + M \Rightarrow KOH + M$
100: $KOH + M \Rightarrow K + OH + M$
101: $K + HO_2 \Rightarrow KOH + O$
102: $KOH + O \Rightarrow K + HO_2$
103: $K + O_2 (+M) \Rightarrow KO_2 (+M)$
104: $KO_2 (+M) \Rightarrow K + O_2 (+M)$
105: $K + H_2O \Rightarrow KO + H_2$
106: $KO + H_2O \Rightarrow KOH + OH$
107: $KOH + OH \Rightarrow KO + H_2O$
108: $KOH + H \Rightarrow K + H_2O$
109: $K + H_2O \Rightarrow KOH + H$
110: $KO_2 + OH \Rightarrow KOH + O_2$
111: $Na + N_2O \Rightarrow NaO + N_2$
112: $NaO + N_2 \Rightarrow Na + N_2O$
113: $NaO + H_2O \Rightarrow NaOH + OH$
114: $NaOH + OH \Rightarrow NaO + H_2O$
115: $NaO + O \Rightarrow Na + O_2$
116: $Na + O_2 \Rightarrow NaO + O$
117: $NaO + NO \Rightarrow Na + NO_2$

dx.doi.org/10.1021/ef3014037 | Energy Fuels 2013, 27, 421−429

Table A1. continued

26: NH + O ⇒ NO + H
27: NH + OH ⇒ HNO + H
28: NH + O_2 ⇒ HNO + O
29: NH + O_2 ⇒ NO + OH
30: NH + NO ⇒ N_2O + H
31: NH + NO ⇒ N_2O + H
32: NH + NO ⇒ N_2 + OH
33: NH + NO_2 ⇒ N_2O + OH
34: NO + O + M ⇒ NO_2 + M
35: NO_2 + M ⇒ NO + O + M
36: NO + OH + M ⇒ HONO + M
37: HONO + M ⇒ NO + OH + M
38: NO + HO_2 ⇒ NO_2 + OH
39: NO_2 + OH ⇒ NO + HO_2
40: NO_2 + H ⇒ NO + OH
41: NO + OH ⇒ NO_2 + H
42: NO_2 + O ⇒ NO + O_2
43: NO + O_2 ⇒ NO_2 + O
44: 2NO + O_2 ⇒ 2NO_2
45: HNO + M ⇒ H + NO + M
46: H + NO + M ⇒ HNO + M
72: N_2H_2 + NO ⇒ N_2O + NH_2
73: N_2O + NH_2 ⇒ N_2H_2 + NO
74: NNH ⇒ N_2 + H
75: NH + NO ⇒ NNH + O
76: NNH + O_2 ⇒ N_2 + HO_2
77: NNH + O_2 ⇒ N_2 + H + O_2
78: NNH + NO ⇒ N_2 + HNO
79: N_2O + M ⇒ N_2 + O + M
80: N_2O + O ⇒ N_2 + O_2
81: O + OH ⇒ H + O_2
82: H + O_2 ⇒ O + OH
83: O + H_2 ⇒ OH + H
84: OH + H_2 ⇒ H_2O + H
85: H_2O + H ⇒ OH + H_2
86: 2OH ⇒ H_2O + O
87: H_2O + O ⇒ 2OH
88: H + O_2 + M ⇒ HO_2 + M
89: HO_2 + M ⇒ H + O_2 + M
90: H + O_2 + N_2 ⇒ HO_2 + N_2
91: HO_2 + N_2 ⇒ H + O_2 + N_2
92: HO_2 + H ⇒ H_2 + O_2
118: Na + NO_2 ⇒ NaO + NO
119: Na + O_2 + M ⇒ NaO_2 + M
120: NaO_2 + M ⇒ Na + O_2 + M
121: Na + OH + M ⇒ NaOH + M
122: NaOH + M ⇒ Na + OH + M
123: NaO + OH ⇒ NaOH + O
124: NaOH + O ⇒ NaO + OH
125: NaO + OH ⇒ Na + HO_2
126: Na + HO_2 ⇒ NaO + OH
127: Na + HO_2 ⇒ NaOH + O
128: NaOH + O ⇒ Na + HO_2
129: NaO + HO_2 ⇒ NaO_2 + OH
130: NaO_2 + O ⇒ NaO + O_2
131: NaO + O_2 ⇒ NaO_2 + O
132: NaO + NH_3 ⇒ NaOH + NH_2
133: NaOH + NH_2 ⇒ NaO + NH_3
134: NaOH + H ⇒ Na + H_2O
135: Na + H_2O ⇒ NaOH + H
136: NaO_2 + OH ⇒ NaOH + O_2
137: NaOH + O_2 ⇒ NaO_2 + OH

AUTHOR INFORMATION

Corresponding Author

*Telephone: +86-10-82544232. Fax: +86-10-62561284. E-mail: xlwei@imech.ac.cn.

Notes

The authors declare no competing financial interest.

ACKNOWLEDGMENTS

Financial support by the Chinese Natural Science Foundation (91130028) is gratefully acknowledged.

REFERENCES

(1) Mahmoudi, S.; Baeyens, J.; Seville, J. P. K. NO_x formation and selective non-catalytic reduction (SNCR) in a fluidized bed combustor of biomass. *Biomass Bioenergy* **2010**, *34*, 1393−1409.

(2) Javed, M. T.; Irfana, N.; Gibbs, B. M. Control of combustion generated nitrogen oxides by selective non-catalytic reduction. *J. Environ. Manage.* **2007**, *83* (3), 251−289.

(3) Niu, S. L.; Han, K. H.; Lu, C. M. An experimental study on the effect of operating parameters and sodium additive on the NO_xOUT process. *Process Saf. Environ. Prot.* **2011**, *89*, 121−126.

(4) Zamansky, V. M.; Lissianski, V. V.; Maly, P. M.; Rusli, D.; Gardiner, W. C. Reactions of sodium species in the promoted SNCR process. *Combust. Flame* **1999**, *117*, 821−831.

(5) Wu, S. H.; Cao, Q. X.; Liu, H.; An, Q.; Huang, X. Experimental and modeling study of the effects of gas additives on the thermal DeNO_x process. *Chin. J. Chem. Eng.* **2010**, *18* (1), 143−148.

(6) Niu, S. L.; Han, K. H.; Lu, C. M. Experimental study on the effect of urea and additive injection for controlling nitrogen oxides emissions. *Environ. Eng. Sci.* **2010**, *27* (1), 47−53.

(7) Zhang, Y. W.; Cai, N. S.; Yang, J. B.; Xu, B. Experimental and modeling study of the effect of CH_4 and pulverized coal on selective non-catalytic reduction process. *Chemosphere* **2008**, *73*, 650−656.

(8) Nimmo, W.; Javed, M. T.; Gibbs, B. M. NO_x control by ammonium carbonate and ammonia with hydrocarbons as additives. *J. Energy Inst.* **2008**, *3*, 131−134.

(9) Perry, R. A.; Miller, J. A. An exploratory investigation of the use of alkali metals in nitrous oxide control. *Int. J. Chem. Kinet.* **1996**, *28*, 217−234.

(10) Lee, S.; Park, K.; Park, J. W.; Kim, B. H. Characteristics of reducing NO using urea and alkaline additives. *Combust. Flame* **2005**, *141*, 200−203.

(11) Yang, W. J.; Zhou, J. H.; Zhou, Z. J.; Chen, Z. C.; Liu, J. Z.; Cen, K. F. Action of oxygen and sodium carbonate in the urea-SNCR process. *Combust. Flame* **2009**, *156*, 1785−1790.

(12) Sandia National Laboratories. *SENKIN: A FORTRAN Program for Predicting Homogeneous Gas Phase Chemical Kinetics with Sensitivity Analysis*; Sandia National Laboratories: Livermore, CA, 1988; SAND87-8248.

(13) http://garfield.chem.elte.hu/Combustion/Combustion.html.

(14) Kovács, T.; Zsély, I. G.; Kramarics, A.; Turányi, T. Kinetic analysis of mechanisms of complex pyrolytic reactions. *J. Anal. Appl. Pyrolysis* **2007**, *79*, 252−258.

(15) Zabetta, E. C.; Hupa, M. A detailed kinetic mechanism including methanol and nitrogen pollutants relevant to the gas-phase combustion and pyrolysis of biomass-derived fuels. *Combust. Flame* **2008**, *152* (1−2), 14−27.

(16) Hindiyarti, L.; Frandsen, F.; Livbjerg, H.; Glarborg, P.; Marshall, P. An exploratory study of alkali sulfate aerosol formation during biomass combustion. *Fuel* **2008**, *87*, 1591−1600.

(17) Launder, B. E.; Sharma, B. I. Application of the energy dissipation model of turbulence to the calculation of flow near a spinning disk. *Lett. Heat Mass Transfer* **1974**, *1*, 131−138.

(18) Magnussen, B. F. Modeling of pollutant formation in gas turbine combustors based on the eddy dissipation concept. *Proceedings of 18th International Congress on Combustion Engines*; Tianjin, China, June 5−8, 1989.

(19) Pope, S. B. Computationally efficient implementation of combustion chemistry using in situ adaptive tabulation. *Combust. Theory Modell.* **1997**, *1*, 41−63.

(20) *Cantera: Object-Oriented Software for Reacting Flows*; http://www.cantera.org.

(21) Lissianski, V. V.; Zamansky, V. M.; Maly, P. M. Effect of metal-containing additives on NO_x reduction in combustion and reburning. *Combust. Flame* **2001**, *125*, 1118−1127.

(22) Li, S.; Wei, X. L. Behavior of alkali metal hydroxides/chlorides for NO reduction in a biomass reburning process. *Energy Fuels* **2011**, *25* (8), 3465−3475.